SUPPORTING INFORMATION

High-Resolution PET Imaging with Therapeutic Antibody-based PD-1/PD-L1 Checkpoint Tracers

Hettich *et al.*

SI MATERIALS AND METHODS

Determination of NOTA molecules per antibody

The number of chelators conjugated to the mAbs was determined as described before, with minor modifications [1]. Briefly, 15 µg Ab (~0.1 nmol) was incubated in ammonium acetate solution (pH 8.2) with varying concentrations of natural Cu^{2+} (0.2–5 nmol) spiked with $^{64}Cu^{2+}$. The nat. Cu^{2+} solutions were prepared by dilution of a copper atomic absorption standard solution (*Trace*CERT, Sigma-Aldrich). After incubation for 1 h at room temperature, labeling samples were equally mixed with diethylenetriaminepentaacetic acid (DTPA; 0.2 g mL^{-1}) and the ratio of mAb-bound and unbound copper was subsequently determined by thin-layer chromatography (TLC) on iTLC SG microfiber paper impregnated with silica gel (Agilent Technologies) using DTPA as the eluent. Unbound Cu^{2+} eluted with the solvent front ($R_f = 1.0$) and Ab-bound activity remained at the origin ($R_f = 0.0$). Radioactivity distribution was measured by phosphorimaging on a Perkin Elmer Cyclone Plus. Determinations were performed in triplicate.

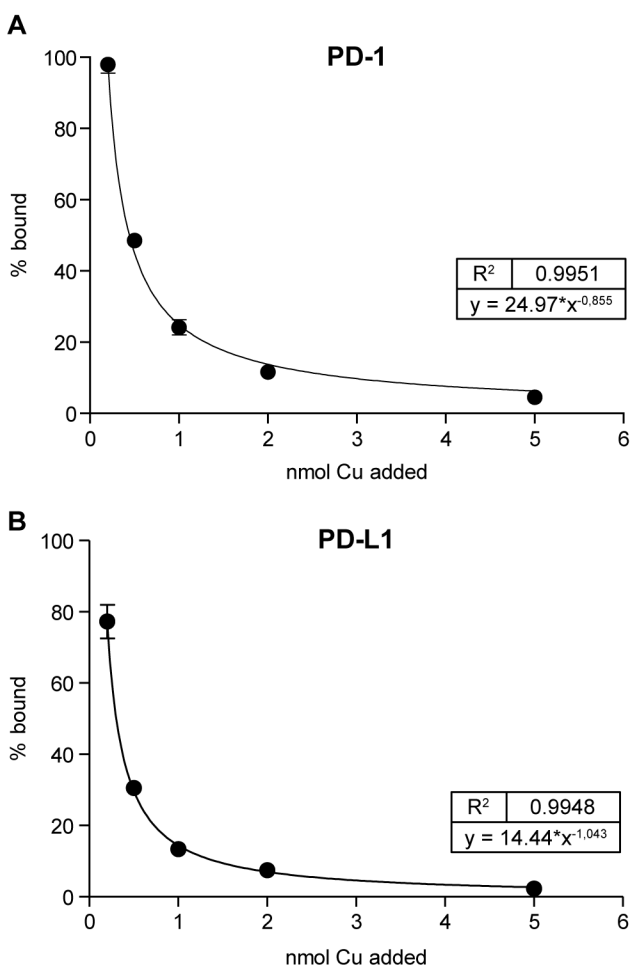**Flow cytometric antibody titration**

Conservation of mAb binding affinity after NOTA conjugation was tested through side-by-side flow cytometric titration of conjugated and unconjugated α-PD-1 and α-PD-L1, respectively. 1×10^6 activated murine CD8 T cells (PD-1) and 1×10^6 IFN-γ-treated B16F10 melanoma cells (PD-L1) were incubated with serially diluted corresponding unconjugated and NOTA-conjugated antibodies (both rat anti-mouse). After washing, cells were stained with fluorochrome-conjugated goat anti-rat IgG mAb (eBioscience) and analyzed with a FACSVerse flow cytometer (BD Biosciences), with the mean fluorescence intensity plotted against the mAb concentration.

Detection of regulatory T cells

Tregs were detected in single-cell suspensions from spleens and lymph nodes of healthy C57BL/6 mice. Cells were first stained for α-CD3, α-CD4 (eBioscience), and α-CD25 (BD Horizon), and subsequently fixed, permeabilized and stained for intracellular FoxP3 with the anti-mouse FoxP3 staining set (eBioscience). Cells were analyzed using a BD FACSVerse flow cytometer with FACSuite software (Becton Dickinson).

1.   Langford JH, Cooper MS, Orchard KH. Development and validation of the 57Co assay for determining the ligand to antibody ratio in bifunctional chelate/antibody conjugates for use in radioimmunotherapy. Nucl Med Biol. 2011; 38: 1103-10.
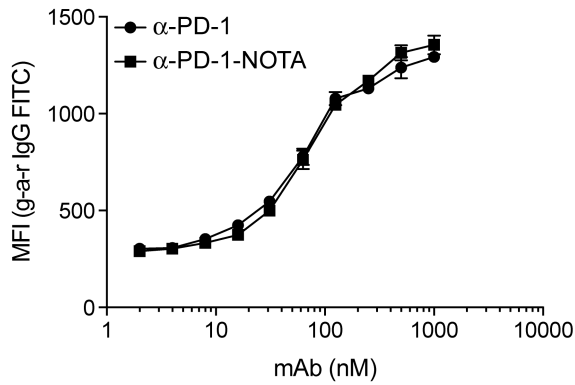
Fig. S1

A

PD-1

R^2 | 0.9951
y = 24.97*x$^{-0.855}$

% bound

nmol Cu added

B

PD-L1

R^2 | 0.9948
y = 14.44*x$^{-1.043}$

% bound

nmol Cu added
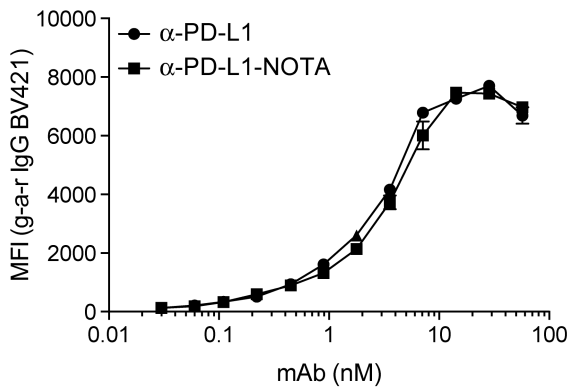
Fig. S1. Determination of NOTA molecules per antibody.

Determination of the degree of NOTA modification per α-PD-1 **(A)** and α-PD-L1 **(B)** antibody molecules. Antibodies were incubated with varying concentrations of copper (0.2–5 nmol) spiked with ^{64}Cu. $n = 3$ experiments each.
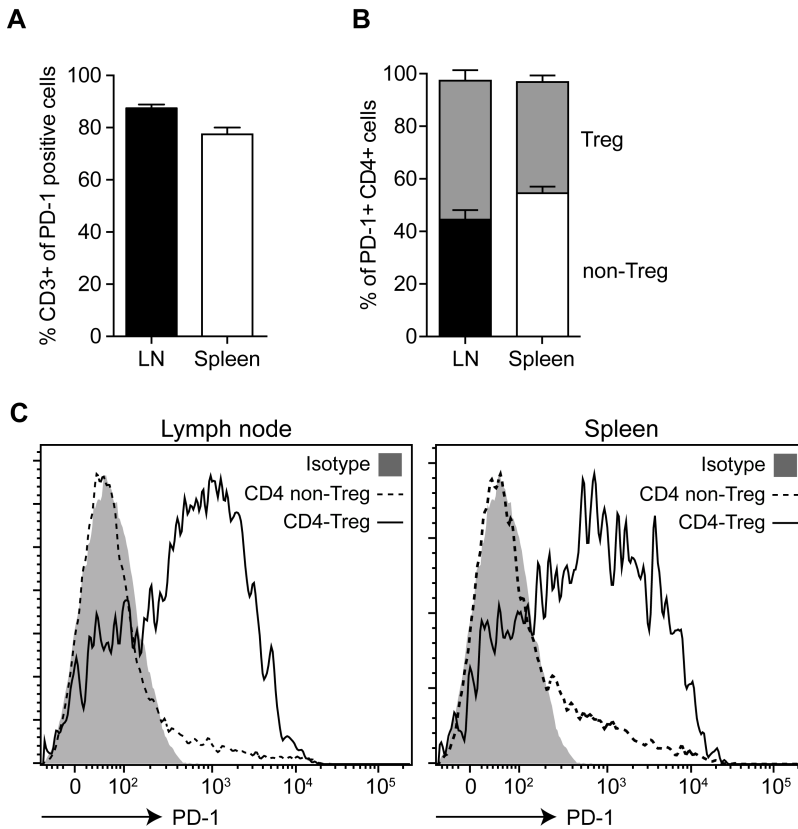
Fig. S2

A

B

Fig. S2. Side-by-side flow cytometric titration.

Titration of NOTA-conjugated vs. unconjugated α-PD-1 **(A)** and α-PD-L1 **(B)**. Serially diluted antibodies were incubated with activated murine T cells (PD-1+) or IFN-γ-treated B16 melanoma cells (PD-L1+) and analyzed as described above. *n* = 3.

Fig. S3

A

B

C

Fig. S3. PD-1 expression on normal and regulatory CD4 T cells in untreated, healthy mice.

(A) The vast majority of PD-1+ cells in lymph nodes and spleen are CD3+ T cells. $n = 3$ mice. **(B)** Tregs and non-Tregs (CD4+ CD25+ FoxP3+) each account for approximately half of the PD-1+ CD4+ cells. $n = 3$ mice. **(C)** Representative histogram overlays of PD-1 expression on Treg and non-Treg CD4 T cells in lymph nodes and spleen.

Fig. S4
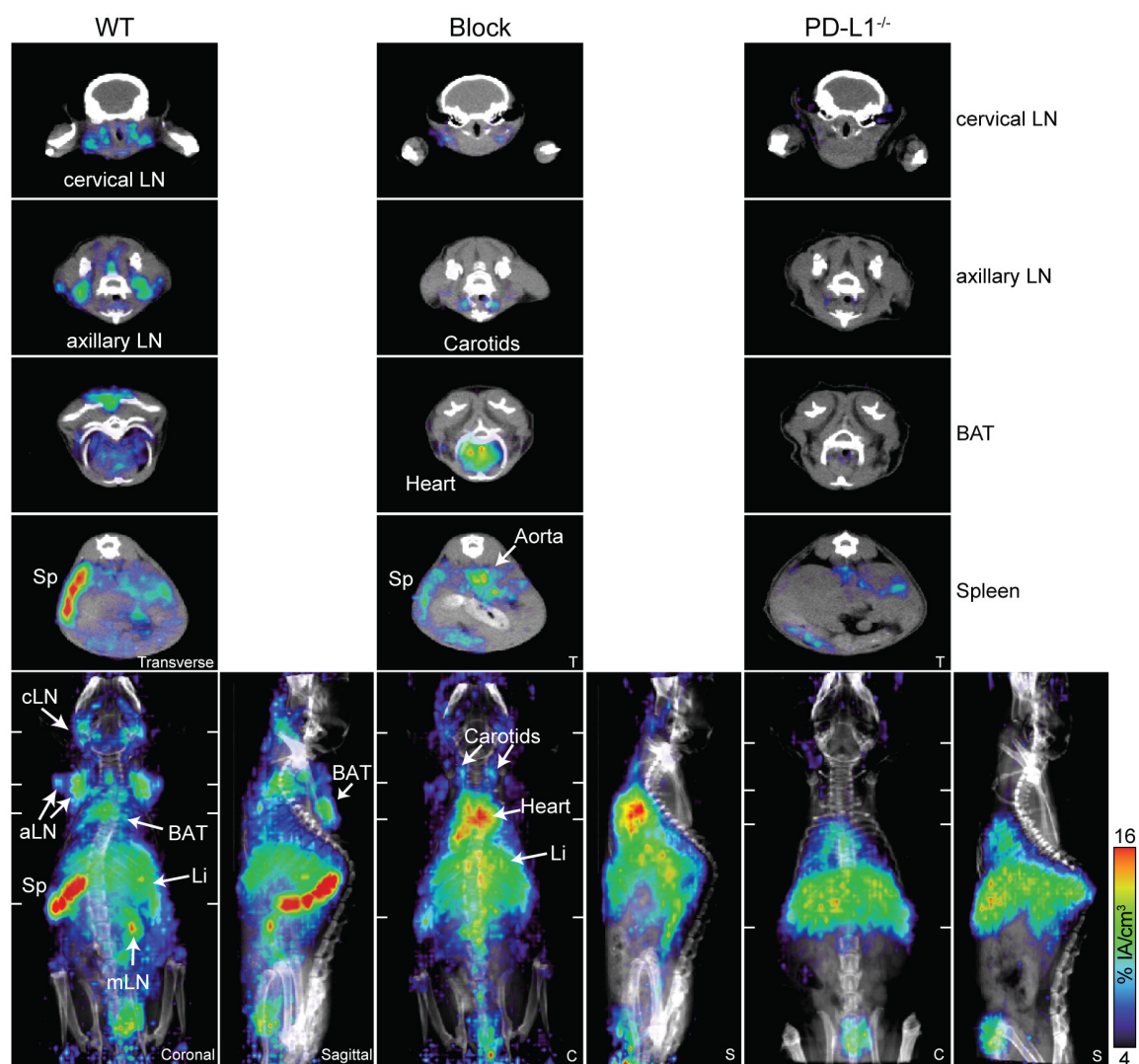
Fig. S4. PD-L1 immunoPET/CT in naive mice

ImmunoPET/CT imaging of ^{64}Cu-NOTA-PD-L1 24 h p.i. with coronal and sagittal whole-body 20-mm maximum intensity projection (MIP) scans shown together with 2-mm transverse MIPs indicated by white ticks.

Abbreviations: cLN – cervical lymph node, aLN – axillary lymph node, mLN – mesenteric lymph node, Li – liver, Sp – spleen, BAT – brown adipose tissue.
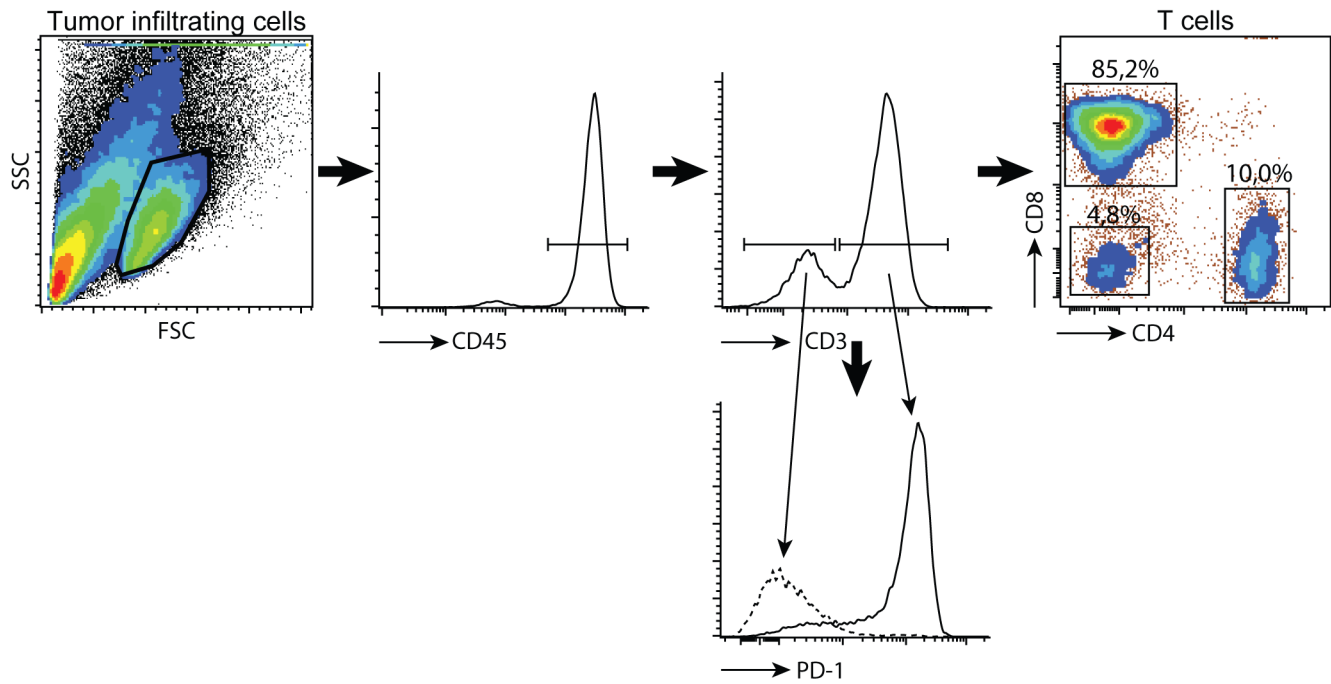
Fig. S5
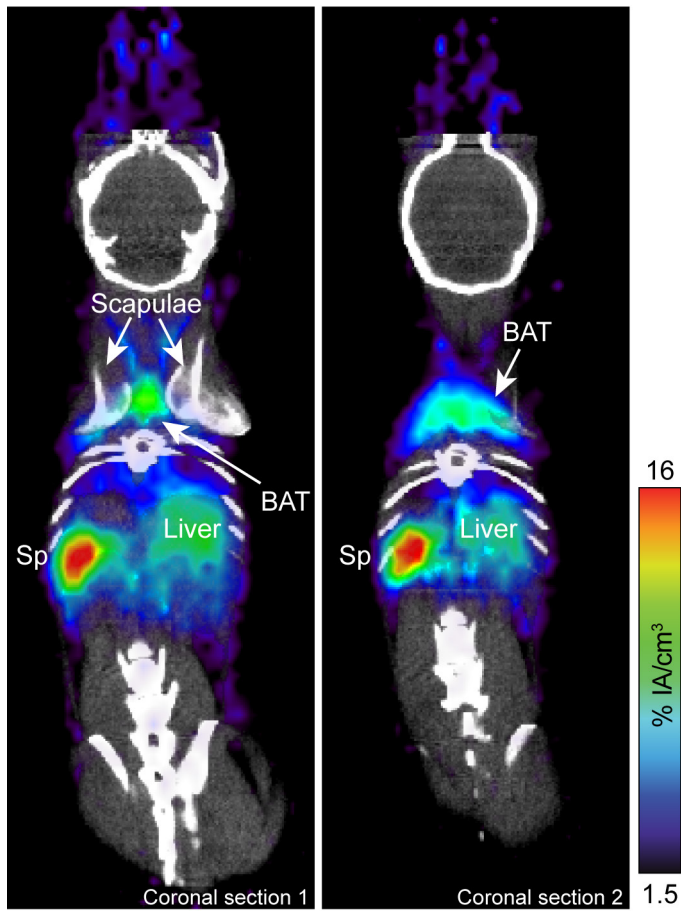
Fig. S5. PD-L1 immunoPET/CT detects interscapular BAT in mice.

Two coronal immunoPET sections of a representative, healthy and untreated WT mouse injected with ^{64}Cu-NOTA-PD-L1 mAb (20 µg; 6.38 ± 0.35 MBq) 24 h p.i. Radiotracer uptake into interscapular butterfly-shaped BAT is indicated by white arrows.

Abbreviations: Sp – spleen, BAT – brown adipose tissue.

Fig. S6

Fig. S6. Strong induction of PD-1^{high} CD8+ TILs by combined immunoradiotherapy.

Flow cytometric analysis of tumor-infiltrating cells 5 days post treatment with tumor radiotherapy (2×12 Gy) and injection of anti-PD-L1 plus anti-CTLA-4. Virtually all tumor-infiltrating cells were CD45+ leukocytes, the majority of which were PD-1^{high} CD3+ T cells. More than 80% of all T cells were CD8+ cytotoxic T cells. Most non-T cells did not show PD-1 expression.

Fig. S7
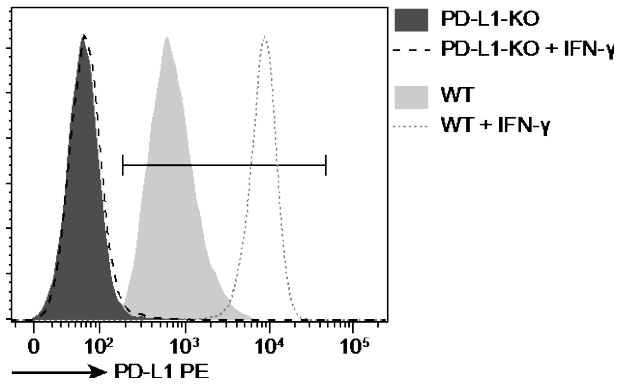
Fig. S7. FACS PD-L1 expression analysis of B16 PD-L1 KO cells generated by CRISPR/Cas9 technology.

PD-L1 KO cells were generated as described in Materials & Methods. WT cells showed weak basal PD-L1 expression, which was strongly upregulated after 24 h of IFN-γ treatment. In contrast, PD-L1 KO cells neither showed basal nor IFN-γ-inducible PD-L1 expression.